Appendix Gap Losses with Pressure-Driven Mass Flows

M. A. Segado, J. G. Brisson

MIT Cryogenic Engineering Lab
Cambridge, MA, USA 02139

ABSTRACT

The clearance space or "appendix gap" between the long pistons and cylinders used in cryogenic expanders plays a key role in the performance of those machines. Losses arising from this gap are well known in the cryogenic and Stirling literature, and result from a combination of fluid flow, pressure fluctuations, and piston motion in the presence of axial temperature gradients. However, most existing analyses of these losses do not include the effects of large, pressure-driven mass flows into and out of the appendix gap and are therefore not applicable to high-pressure-ratio cryogenic expanders.

To overcome some of the limitations of existing models, a new analysis was carried out which considers the effects of large, pressure-driven mass flows concurrently with the effects of large pressure fluctuations in the gap, cyclic piston motion, and transient conduction in both the piston and cylinder in addition to all first-order cross terms. The resulting analytical expression agrees with existing literature for heat transfer due to piston motion alone ("shuttle heat transfer") and supplements it with four additional terms describing the effects of fluid motion and pressure fluctuations as well as their interaction with piston motion.

The new appendix gap analysis was further extended to yield a complete model of the appendix gap. Since fluid density and material properties of the piston and cylinder are strong functions of temperature, one-dimensional numerical integration was used in conjunction with a shooting method to solve for the approximate temperature, heat transfers, mass flows, and pressure variations as a function of axial position along the piston, along with an estimate of the temperature of fluid exiting the gap for use in cryocooler models. The appendix gap model predicts a minimum gap loss for intermediate gap sizes as well as highly non-linear temperature profiles at large gap widths, and was successfully applied to examine design tradeoffs in a model of a high-pressure-ratio cryocooler.

INTRODUCTION

A variety of applications exist for piston-cylinder machines, and in many cases (e.g. cryogenic expanders and Stirling engines) such machines must span a significant axial temperature difference. As axial heat transfers are often detrimental to the performance of expanders and other such devices, care must be taken in modeling the various heat transfer mechanisms at work. This seems particularly true of the heat and enthalpy transfers in the clearance space between a piston and cylinder; such spaces are typically sealed at the room-temperature end only

Cryocoolers 17, edited by S.D. Miller and R.G. Ross, Jr.

and are called "appendix gaps" in the cryogenic and Stirling literature. Existing models of such appendix gap heat transfers, however, do not include the effects of large, pressure-driven mass flows and are therefore not applicable to high-pressure-ratio (HPR) cryogenic expanders. The present work presents a preliminary model suitable for such expanders.

Heat and enthalpy transfers in or around the appendix gap arise from at least four conceptually-distinct mechanisms: 1) axial conduction through the piston and cylinder walls, 2) gas blow-by or seal leakage, 3) "shuttle" heat transfers, and 4) gas enthalpy transfers. The first of these occurs when axial temperature gradients drive axial heat transfers via pure conduction. The second arises when pressure differences between the two ends of the piston force fluid past imperfect piston/cylinder seals, but was not considered in the present work. The remaining mechanisms are somewhat more complicated and will be described in detail below.

Shuttle Heat Transfer

Shuttle heat transfers result from the relative motion of a piston and cylinder in the presence of an axial temperature gradient. As illustrated in Figure 1, the piston receives a heat transfer from the cylinder wall near the warm end of its stroke but deposits this heat transfer near the cold end of its stroke, physically "shuttling" thermal energy from the hotter end of the apparatus to the colder end.

The shuttle heat transfer mechanism has been know at least as far back as 1959, when McMahon and Gifford referred to "motional heat transfer" in their description of what is now the Gifford-McMahon refrigerator.[1] Many analyses of the loss exist in the literature; one of the most useful is that of Chang and Baik, who derived a simple expression for the loss by treating the piston and cylinder walls as semi-infinite solids with linear axial temperature profiles and neglecting the motion and heat capacity of fluid in the intermediate gap.[2] The expression is reproduced here in a slightly modified form:

$$\dot{Q}_{\text{shuttle}} = -\left(\frac{T_{\text{warm}} - T_{\text{cold}}}{L_{\text{pis}}}\right)\frac{\pi D S^2 k_{\text{gap}}}{8\delta_{\text{gap}}}\frac{b_{\text{pis}} + b_{\text{cyl}} + 1}{\left(b_{\text{pis}} + b_{\text{cyl}}\right)^2 + \left(b_{\text{pis}} + b_{\text{cyl}} + 1\right)^2}, \tag{1}$$

where T_{warm} and T_{cold} are the mean temperatures of the cylinder's warm end and cold end, respectively, L_{pis} is the piston length, D is the expander diameter, S is the stroke length of the piston, k_{gap} is the thermal conductivity of the fluid in the appendix gap, δ_{gap} is the width of the appendix gap, and b_{pis} and b_{cyl} are Biot numbers with a characteristic length equal to the thermal penetration depth into the solids. More specifically, the Biot numbers are given by equation (2), where k_{pis} or k_{cyl} and α_{pis} or α_{pis} are the thermal conductivities and thermal diffusivities of the piston or

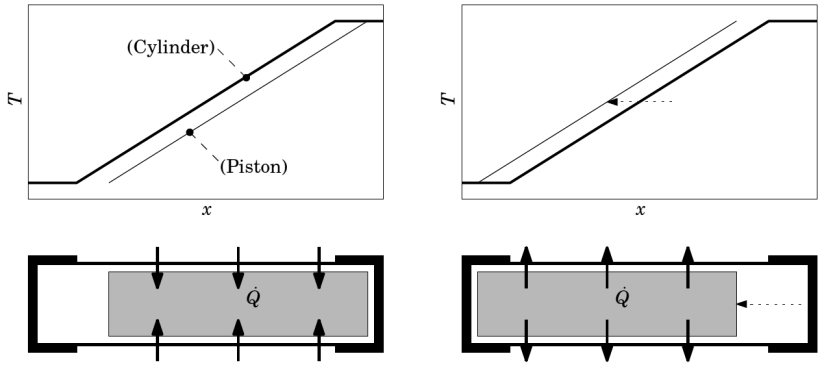

Figure 1. Illustration of shuttle heat transfer. While near the warm end of the expander, the piston receives a heat transfer from the locally-warmer cylinder walls; it then carries the thermal energy toward the cold end before transferring it back to the cylinder. The net heat thus transported is proportional to the square of the piston's stroke length. (Figure from reference 6, used with permission.)

cylinder, respectively, and ω is the angular frequency of operation of the expander:

$$b_{\text{pis}} = \frac{\left(k_{\text{gas}}/\delta_{\text{gap}}\right)}{k_{\text{pis}}}\sqrt{\frac{\alpha_{\text{pis}}}{2\omega}}, \quad b_{\text{cyl}} = \frac{\left(k_{\text{gas}}/\delta_{\text{gap}}\right)}{k_{\text{cyl}}}\sqrt{\frac{\alpha_{\text{cyl}}}{2\omega}}. \tag{2}$$

The expression predicts that shuttle heat transfer scales linearly with axial temperature gradient but quadratically with the piston's stroke length. Narrower gaps also increase the heat transfer, though only when the Biot numbers are small (for large Biot numbers the heat transfer is dominated by transient conduction effects in the solids and the gap width has little effect).

Gas Enthalpy Transfer

In addition to the energy carried by the reciprocating piston, fluid motion in the appendix gap also yields a net enthalpy transfer in the presence of axial temperature gradients. This gas enthalpy transfer (or "GET") can be either detrimental or favorable depending on the relative phase between the pressure fluctuations and piston motion. Unlike the shuttle heat transfer loss described above, however, GET losses tend to favor narrower appendix gaps as these reduce the amount of mass flow. Consequently, the net appendix gap loss is typically minimized for intermediate gap widths.

The literature surrounding gas enthalpy transfer (which is occasionally referred to as "pumping loss") is considerably less developed that that of shuttle heat transfer. The first analysis appears to have been introduced by Ríos in a 1969 doctoral thesis; Ríos treated the loss separately from shuttle heat transfer, and assumed that temperature difference between fluid entering and exiting the appendix gap was a result of the piston's motion changing the mean gap temperature.[3] Several analyses surfaced between 1969 and 1986,[a] though in the past 25 years the only analytical treatment in the open literature appears to be Kotsubo and Swift's 2006 thermoacoustic analysis of "displacer gap loss".[4] Notably, this was also the only analysis surveyed that included the effects of large pressure fluctuations and pressure-driven flows on the local heat transfer (though an analysis extending this to the entire gap was not presented). The local heat transfer expressions developed by Kotsubo and Swift are considerably more complicated than those presented here, but they are also much more general and should be a good resource when the assumptions in the analysis presented below cannot be safely made.

ANALYSIS

Including the gas enthalpy transfer loss in an appendix gap model poses an interesting challenge. Mass flows in the gap give rise to substantial heat transfers with the piston and cylinder walls and are therefore instrumental in determining the axial temperature profile of the gap. However, the amount of mass flow depends not only on the pressure fluctuations but also on the axial temperature profile (via the fluid's density). The matter is further complicated by temperature-dependent fluid properties and the desire to create a model efficient enough for use in design-space explorations.

The appendix gap loss analysis in this work seeks to overcome the modeling difficulties above while still yielding a computationally-light model for use in expander simulations. To this effect, a hybrid of analytical and numerical approaches was used: an analytical "local" solution was found to relating heat and enthalpy transfers to temperature gradients, fluid flows, and pressure fluctuations at a given axial position in the expander, and a numerical "global" procedure extending the local solution to an entire appendix gap (complete with position-dependent mass flows, temperature-dependent material properties, and a non-linear axial temperature profile). Several simplifying assumptions were made:

1. End effects are negligible.

[a] A more thorough survey of the gas enthalpy transfer literature is included in Segado's master's thesis.

2. Velocities, temperatures, and pressures all vary sinusoidally.
3. The axial temperature gradient is locally linear over a distance of one stroke length and is identical in the piston, cylinder, and fluid.
4. Material and fluid properties are uniform over a distance of one stroke length.
5. Material and fluid properties at a given axial position are constant at their time-averaged mean values (including fluid density).
6. The working fluid may be modeled as an ideal gas.
7. The penetration depth of heat transfer into the piston and cylinder walls is much smaller than the wall thicknesses and expander diameter; both walls may therefore be modeled as planar semi-infinite solids.
8. The gap width is much smaller than the expander diameter such that curvature effects may be neglected.
9. The gap is of uniform width and is perfectly sealed at the warm end (e.g., by means of an O-ring or ideal clearance seal).
10. In the First Law for fluid in the gap, viscous dissipation and pressure gradients are negligible compared to other terms.
11. Fluid flow is laminar, hydrodynamically fully developed, and thermally fully developed.
12. Pressure-driven Poiseuille flow dominates in the gap; Couette flow due to piston motion is small in comparison.

These assumptions are mostly consistent with those in the literature. The notable exception is assumption 12, which is expected to be valid in an HPR expander with large pressure-driven mass flows and a low operating frequency.

Both the piston-cylinder seal and the open end of the appendix gap are assumed to move with the piston in the present work; all analyses were therefore carried out in the reference frame of the piston to avoid dealing with moving boundary conditions at the ends of the gap.

Local Analytical Solution

The first part of the gap loss analysis aims to find a relationship between the temperature gradient, mean fluid velocity, pressure fluctuations, and material properties at a given axial position in the expander. Conservation of mass is addressed first, beginning by applying the mass conservation to a differential slice of the gap:

$$\frac{\partial}{\partial t} dm(x,t) = \dot{m}(x,t) - \dot{m}(x+dx,t). \tag{3}$$

Substituting for m using the ideal gas property constitutive relation and taking the limit as dx approaches zero,

$$\frac{\partial \dot{m}(x,t)}{\partial x} = \left(\frac{\pi D \delta}{RT(x)} \right) \frac{\partial P(x,t)}{\partial t}. \tag{4}$$

Momentum conservation may be addressed by rearranging the widely-available solution for pressure drop in planar Poiseuille flow. In conjunction with the ideal gas property constitutive relation, this yields

$$\frac{\partial P(x,t)}{\partial x} = \left(\frac{-12RT(x)\mu(T)}{\pi D \delta^3 P(x,t)} \right) \dot{m}(x,t). \tag{5}$$

Equations (4) and (5) are coupled non-linear PDEs. To make these more tractable, the time-

variant pressure $P(x,t)$ in the denominator of (5) may be replaced with a time-invariant mean pressure $P_{\text{mean}}(x)$, effectively ignoring the effect of cyclic density variations on the flow. A geometric mean was used as this is expected to better capture the effects large pressure fluctuations.

The procedure used to address energy conservation is somewhat more involved than that used for mass and momentum conservation. First, the heat equations for the piston and cylinder may be simplified to

$$\frac{\partial T_d}{\partial t} = \alpha_d \frac{\partial^2 T_d}{\partial y_d^2} \quad \text{and} \quad \frac{\partial T_c}{\partial t} = \alpha_c \frac{\partial^2 T_c}{\partial y_c^2}, \tag{6}$$

respectively, by applying the assumptions stated earlier. The (thermal) energy equation for the fluid may similarly be simplified to

$$\rho_0 c_P \frac{\partial T}{\partial t} + \rho_0 c_P u(y) \frac{\partial T}{\partial x} = k \frac{\partial^2 T_c}{\partial y_c^2} + \frac{\partial P}{\partial t}. \tag{7}$$

In the case when the gap is substantially thinner than the characteristic thermal penetration depth into the fluid (such that $\delta^2 \ll \alpha / \omega$), the first term of equation (7) is negligible.

The cyclic-steady-state solution of the governing equations above may be found by using separation of variables. The temperatures (to first order in x), pressure, fluid velocity, and cylinder motion (in the stationary-piston reference frame) are first expressed in terms of complex exponentials, viz.:

$$T = \text{Re}\left[A(y) e^{i\omega t} + T_0 + \Gamma (x - x_0) \right], \tag{8}$$

$$P = \text{Re}\left[\frac{\Delta P}{2} e^{i\omega t} e^{i\phi} + P_0 \right], \tag{9}$$

$$u = \text{Re}\left[6U \frac{y}{\delta} \left(1 - \frac{y}{\delta} \right) e^{i\omega t} \left(-i e^{i\phi} \right) \right], \tag{10}$$

$$x_c = -x_d = \text{Re}\left[\frac{-S}{2} e^{i\omega t} \right]. \tag{11}$$

Several new variables have been introduced above. In order, $A(y)$ is the complex amplitude of the solid or fluid temperature profile, Γ is the local axial temperature gradient, ΔP is the complex pressure amplitude at a given axial location, ϕ is the phase lead of the cold-end pressure (measured relative to that in a gas spring with identical piston motion), P_0 is the average pressure of the expander, and U is the complex bulk velocity amplitude.

Substituting expressions (8)–(11) above into the energy equations (6) and (7) and removing the real-part operators transforms those PDEs into much simpler ODEs. Solving these yields the complex temperature amplitude in the piston and cylinder, respectively,

$$A_d(y_d) = C_1 e^{(1+i)\sqrt{\frac{\omega}{2\alpha_d}} y_d} + C_2 e^{-(1+i)\sqrt{\frac{\omega}{2\alpha_d}} y_d}, \tag{12}$$

$$A_c(y_c) = C_3 e^{(1+i)\sqrt{\frac{\omega}{2\alpha_c}} y_c} + C_4 e^{-(1+i)\sqrt{\frac{\omega}{2\alpha_c}} y_c}, \tag{13}$$

as well as the complex temperature amplitude profile in the fluid,

$$A(y) = \frac{-i e^{i\phi}}{k} \left[\frac{\omega \Delta P y^2}{4} - U \rho_0 c_P \Gamma \frac{y^3}{\delta} \left(1 - \frac{y}{2\delta} \right) \right] + C_5 y + C_6. \tag{14}$$

A total of six boundary conditions govern the temperature profiles in the piston, cylinder, and fluid. First, the temperatures deep within the solid piston and cylinder walls are known;

$$A_d(+\infty) \to 0, \tag{15}$$

$$A_c(-\infty) \to \frac{-\Gamma S}{2}. \tag{16}$$

Additionally, the piston and cylinder surfaces must be at the same temperature as the fluid that they contact:

$$A_d(0) = A(0), \tag{17}$$

$$A_c(0) = A(\delta). \tag{18}$$

Finally, the heat flux out of the piston surface must equal that into the contacting fluid (and likewise for the heat flux out of the displacer):

$$-k_d \left.\frac{dA_d}{dy_d}\right|_{y_d=0} = -k \left.\frac{dA}{dy}\right|_{y=0}, \tag{19}$$

$$-k_c \left.\frac{dA_c}{dy_c}\right|_{y_c=0} = -k \left.\frac{dA}{dy}\right|_{y=\delta}. \tag{20}$$

When evaluated using the ODE solutions (12)–(14), the six boundary conditions form a system of six equations with six unknowns (C_1–C_6). These coefficients may be found and back-substituted into (14) to yield an expression for the complex temperature amplitude of the fluid:

$$\begin{aligned} A(y) = {} & \frac{-ie^{i\phi}}{k}\left[\frac{\omega \Delta P y^2}{4} - U\rho_0 c_P \Gamma \frac{y^3}{\delta}\left(1 - \frac{y}{2\delta}\right)\right] \\ & + \frac{\theta}{\beta\delta}\left[\frac{ie^{i\phi}\delta^2}{2k}\left(\frac{\omega\Delta P}{2} - U\rho_0 c_P \Gamma\right)\left(i + 2b_d(1+i)\right) + \frac{\Gamma S}{2} i\right] y \\ & + b_c \frac{\theta}{\beta}\left[\frac{ie^{i\phi}\delta^2}{2k}\left(\frac{\omega\Delta P}{2} - U\rho_0 c_P \Gamma\right)\left(4b_d + 1 + i\right) + \frac{\Gamma S}{2}(1+i)\right] - \frac{\Gamma S}{2}, \end{aligned} \tag{21a}$$

where for readability

$$\beta \equiv (b_c + b_d)^2 + (b_c + b_d + 1)^2, \quad \theta \equiv (b_c + b_d) - i(b_c + b_d + 1). \tag{21b}$$

With the temperature profile known it is now possible to find the total enthalpy transfer rate in the axial direction. This may be broken up into four components: 1) the heat transfer due to axial conduction through the piston and cylinder walls, 2) the enthalpy carried by the fluid, 3) the thermal energy carried by the cylinder wall's motion, and 4) the mechanical work transfer in excess of piston *PdV* work carried by the reciprocating cylinder wall.[b] The first of these terms is straightforward and may be found by multiplying the cross-sectional areas of the piston and cylinder by their thermal conductivities and the axial temperature gradient:

$$\dot{Q}_{d,c} = \pi D \Gamma (k_d \delta_d + k_c \delta_c). \tag{22}$$

The second term may be found by integrating $\rho_0 c_P u(t,y) T(t,y)$ over the cross-sectional area of the gap and then integrating again over a cycle find the average value:

$$\overline{\dot{H}} = \frac{\omega}{2\pi} \int_0^{2\pi/\omega} \left(\int_0^{\delta} \rho_0 c_P u(t,y) T(t,y) \pi D dy \right) dt. \tag{23}$$

[b] The *PdV* work of a piston-cylinder device is by convention not considered part of the appendix gap enthalpy transfer. The excess work transfer term will be much smaller than the overall *PdV* work but is included for consistency between the chosen reference frame and the typical stationary reference frame used in the literature.

The third term may be found by integrating the heat flux into the cylinder wall to find the thermal energy per unit surface area, multiplying this by both velocity and circumference to find the enthalpy transfer rate, and finally integrating over a cycle find the average value:

$$\overline{\dot{H}_c} = \frac{\omega}{2\pi}\int_0^{2\pi/\omega}\left(\int k\left.\frac{dT}{dy}\right|_{y=0} dt\right)\pi D u(t,y)\,dt\,. \tag{24}$$

The fourth term may be found by noting that the tension in by the cylinder wall is equal to the force on the piston plus the force on the appendix gap cross section, the latter given by $(\pi D\delta)\cdot P(t)$. The desired excess work may therefore be found by multiplying this appendix gap force by the cylinder wall's velocity and integrating to average over a cycle:

$$\overline{\dot{W}_c} = \frac{\omega}{2\pi}\int_0^{2\pi/\omega} -\pi D\delta P(t)u_c(t)\,dt\,. \tag{25}$$

Evaluating equations (22)–(25) and simplifying yields the time-averaged appendix gap enthalpy transfer rate from all sources:

$$\begin{aligned}\dot{Q}_{d,c} + \overline{\dot{H}} + \overline{\dot{H}_c} + \overline{\dot{W}_c} = \pi D\Bigg\{&\Gamma\frac{S^2 k}{8\delta}\left(\frac{b_c+b_d+1}{\beta}\right)\\ &+\Gamma\left(k_d\delta_d + k_c\delta_c\right)\\ &+\Gamma\frac{(\rho_0 c_P U)S\delta}{4}\left(\frac{(b_c-b_d)\cos\phi}{\beta}\right)\\ &+\frac{\omega\Delta P S\delta}{16}\left(\frac{(b_d-b_c)\cos\phi+\left[4b_c\left(b_c+b_d+\frac{3}{4}\right)+b_d+1\right]\sin\phi}{\beta}\right)\\ &+\Gamma\frac{(\rho_0 c_P U)^2\delta^3}{4k}\left(\frac{(b_c+b_d)\left[(2b_c+1)(2b_d+1)+\frac{1}{2}\right]+\frac{1}{2}}{\beta}-\frac{9}{35}\right)\\ &-\frac{\omega\Delta P(\rho_0 c_P U)\delta^3}{8k}\left(\frac{(b_c+b_d)\left[(2b_c+1)(2b_d+1)+\frac{1}{2}\right]+\frac{1}{2}}{\beta}-\frac{3}{10}\right)\Bigg\}.\end{aligned} \tag{26}$$

Note that the first term of the solution is identical to the pure shuttle heat transfer (1) presented by Chang and Baik. The additional terms in the solution capture the effects of pressure fluctuations and fluid flow as well as their various interactions, save for the second term which represents axial conduction in the piston and cylinder walls.

Finally, the PDEs for pressure and mass flow shown earlier may also be transformed into ODEs using the same type of complex variable substitution:

$$\frac{d\dot{M}(x)}{dx} = \left(\frac{-i\omega\pi D\delta}{2RT(x)}\right)\Delta P(x), \tag{27}$$

$$\frac{d\Delta P(x)}{dx} = \left(\frac{-24RT(x)\mu(T)}{\pi D\delta^3\overline{P}}\right)\dot{M}(x). \tag{28}$$

Global Numerical Solution

The local solution above requires knowledge of the highly position-dependent fluid mass flow rate amplitude (which is largest near the open end of the gap and zero at the seal). The mass flow, however, depend on the axial temperature profile as mentioned earlier. The circular dependency was addressed in this work by combining numerical integration with a shooting method as detailed below.

The temperature gradient at any axial position in the gap may found in terms of the local temperature, pressure amplitude, and flow amplitude by rearranging equation (26),

$$\Gamma = \frac{\overbrace{\left(\dot{Q}_{d,c} + \overline{\dot{H}} + \overline{\dot{H}_c} + \overline{\dot{W}_c}\right)}^{\text{Constant along gap length}} - f\left(T, \Delta P, U, \ldots\right)}{g\left(T, \Delta P, U, \ldots\right)}, \tag{29}$$

where $f(\,)$ and $g(\,)$ are lengthy but closed-form functions of the quantities at a given axial position. Equations (27), (28), and (29) now form a system of three coupled non-linear ODEs which may be solved by numerical integration. Guesses are first provided for the total gap loss and the mass flow amplitude at the open end of the gap, and these are adjusted by a gradient-search algorithm until the computed temperature at the sealed end of the gap equals an imposed boundary condition and the computed mass flow amplitude at the sealed end equals zero.

For simplicity, the present version of the model assumes that the phase shift is essentially independent of position; this corresponds physically to an appendix gap that offers little flow resistance other than that of the seal itself. This approximation seems reasonable for cryogenic machinery where the volume of the gap is expected to be negligible for gaps thin enough to offer a significant flow resistance.

The solution approach outlined above was implemented in MATLAB using the included non-stiff *ode45* equation solver. Several additional outputs were provided from the model for use in an expander simulation code as described briefly by Segado, Hannon, and Brisson and in more depth by Segado.[5,6]

PRELIMINARY RESULTS

The model in this work was initially intended as a subcomponent of the higher-level expander simulation mentioned above and has undergone limited testing as a stand-alone unit. Nevertheless, qualitative results from both the expander simulations and cursory stand-alone testing show promise; this section will focus on the latter as details of the expander simulations are reported elsewhere.

Overall Breakdown of Loss Mechanisms

Figure 2 shows a breakdown of the appendix gap losses as a function of appendix gap width for a typical cryogenic expander; in this figure, shuttle heat transfer is defined as the energy transfer carried by the moving cylinder wall and GET is defined as the energy carried by the moving fluid. Note also that the losses shown have been averaged along the expander length as the actual breakdown is strongly dependent on axial position. The qualitative behavior of the model demonstrates the expected trends: shuttle heat transfer dominates the loss for narrow gaps while gas enthalpy transfer dominates for wide gaps, yielding a minimum loss at an intermediate gap width.

Interestingly, the shuttle heat transfer terms become *beneficial* when the gap width is sufficiently large (above 0.45 mm for this example). This is reflected in the size of the total, which for the largest gaps is smaller than the gas enthalpy transfer component alone. The reversal of shuttle may stem from the effect of pressure-driven heat transfers. For a cryogenic expander, pressure fluctuations force heat transfers into the piston nearer to the cold end of its stroke (during compression of the working fluid) and out of the piston nearer to the warm end of its stroke (during expansion). The net effect of these pressure-driven heat transfers into the piston is therefore an enthalpy transfer from the cold end to the warm end.

While the shuttle heat transfer as defined above does indeed become negative for large gaps, it is important to keep this result in the context of the other losses as the distinction between shuttle and GET depends on the chosen reference frame. In a stationary-piston reference frame, for example, the pressure-driven heat transfer described above appears to have the opposite

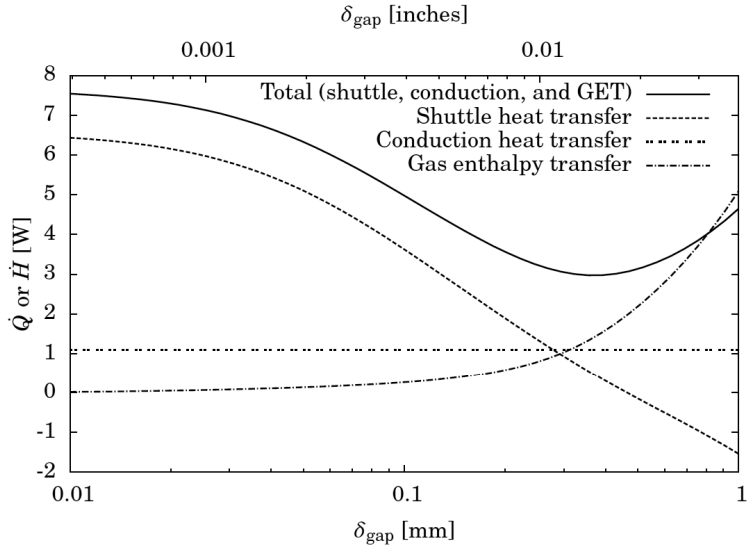

Figure 2. Sample breakdown of loss mechanisms (axially averaged along the length of the appendix gap) as a function of appendix gap width. The overall trends match the expected behavior: shuttle heat transfers are decrease for wider gaps while gas enthalpy transfer increases, yielding a minimum total loss at an intermediate gap width. Note that caution should be exercised when interpreting loss breakdowns like that shown in the figure as the breakdown is actually a function of the chosen reference frame.

effect; namely, heat transfers are forced into the cylinder walls near the warm end of their "stroke" and drawn out near the cold end, contributing a net-*detrimental* enthalpy transfer.

Axial Dependence of Losses and Temperature

The breakdown between losses, in addition to providing some information about the losses throughout the entire gap as above, may also be used to illustrate the variation in loss modes as a function of axial position (Figure 3a). Perhaps most interesting is the position sensitivity of the tradeoff between GET and the other losses. As the appendix gap is made wider, an increasing fraction of the gap (beginning at the open end) is dominated by gas enthalpy transfer while the portion dominated by shuttle is relegated to an ever-shorter section near the sealed end.

The behavior above may be further understood by looking at the axial temperature profile (Figure 3b). For sufficiently wide gaps, fluid flows isothermalize the region near the gap's open end and shift the temperature gradients toward the sealed end of the expander where mass flows are lower. In a cryogenic expander this behavior places much of the gap fluid near the cold-end temperature, yielding a higher mean fluid density and greater mass flow rates than would be expected were the temperature profile linear. The thermodynamic cycle executed by expander is likely to suffer as a result of this higher "dead mass".

Finally, Figure 3b also demonstrates the effects of material property variations in the narrow-gap regime when GET is insignificant: as the thermal conductivity of the fluid, the piston, and the cylinder all decrease with temperature, the resistance to conduction and shuttle heat transfers is higher near the cold end yielding a considerably steeper temperature gradient in that region.

CONCLUSIONS AND FUTURE WORK

Of the work presented above, two points stand out as particularly notable. First, the predicted temperature profile becomes quite non-linear when pressure-driven flows and material prop-

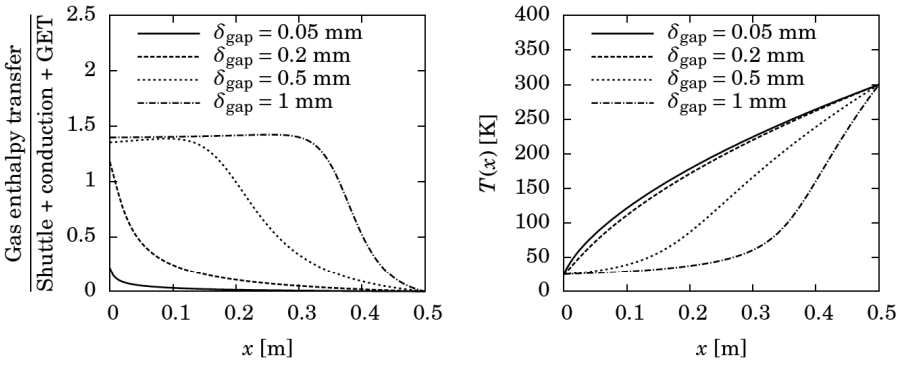

Figure 3. Axial position-dependence of (a) the ratio of GET to the total loss and (b) temperature along the expander. As the gap becomes wider gas enthalpy transfers penetrate further into the gap, isothermalizing an increasing fraction of the gap's length. Other modes of energy transfer (e.g., shuttle) continue to prevail near the warm end of the gap where mass flows are smaller.

erty variations are considered (the latter including the temperature-dependent density and thermal conductivity of the gas and the temperature-dependent heat capacity and thermal conductivity of the walls). Such nonlinearity has the potential to affect both the total appendix gap heat transfer and the amount of mass flow entering and exiting the gap over a cycle. In the case of a cryogenic expander, both effects can be detrimental to the machine's efficiency.

Second, the distinction on what is shuttle heat transfer and what is gas enthalpy transfer is entirely dependent on the chosen reference frame. The total effective heat transfer does not depend on the choice of reference frame and exhibits a minimum as a function of the piston-cylinder gap.

Many opportunities exist for extending the present work; for example, the effects of piston and cylinder material, working fluid choice, operating frequency, or pressure ratio could be examined in more detail. On a more fundamental level, equation (26) could be non-dimensionalized and a thorough order-of-magnitude analysis performed in an effort to either simplify the equation or gain insight into the different regimes present (i.e., the conditions under which each term dominates and the resulting response of the system to the different design parameters). Finally, experimental or CFD validation could prove both interesting and useful.

REFERENCES

1. McMahon, H.O. and Gifford, W.E., "A New Low-Temperature Gas Expansion Cycle—Part I," *Advances in Cryogenic Engineering 5*, Plenum Press, New York (1960), pp. 354–367.
2. Chang, H.-M. and Baik, J.H., "An Exact Expression for Shuttle Heat Transfer," *Advances in Cryogenic Engineering 41*, Plenum Press, New York (1996), pp. 1535–1542.
3. Ríos, P.A., *An Analytical and Experimental Investigation of the Stirling Cycle*, Doctoral thesis, Massachusetts Institute of Technology, Cambridge (1969).
4. Kotsubo, V. and Swift, G., "Thermoacoustic Analysis of Displacer Gap Loss in a Low Temperature Stirling Cooler," *Advances in Cryogenic Engineering 51*, American Institute of Physics, Melville (2006), pp. 353–360.
5. Segado, M.A., Hannon, C.L., and Brisson, J.G., "Losses and Related Design Tradeoffs in Floating Piston Expanders," present proceedings.
6. Segado, M.A., *Analysis and Mitigation of Key Losses in a Multi-Stage 25–100 K Cryocooler*, Master's thesis, Massachusetts Institute of Technology, Cambridge (publication expected 2012).